

CHEMISTRY

A EUROPEAN JOURNAL

Supporting Information

© Copyright Wiley-VCH Verlag GmbH & Co. KGaA, 69451 Weinheim, 2010

Electrochemical Synthesis and Characterisation of Alternating Tripyridyl–Dipyrrole Molecular Strands with Multiple Nitrogen-Based Donor–Acceptor Binding Sites

Alexandra Tabatchnik-Rebillon,^[a] Christophe Aubé,^[a] Hicham Bakkali,^[a] Thierry Delaunay,^[a] Gabriel Thia Manh,^[a] Virginie Blot,^[a] Christine Thobie-Gautier,^[a] Eric Renault,^[a] Marine Soulard,^[a] Aurélien Planchat,^[a] Jean-Yves Le Questel,^[a] Rémy Le Guével,^[b] Christiane Guguen-Guillouzo,^[b] Brice Kauffmann,^[c] Yann Ferrand,^[c] Ivan Huc,^[c] Karène Urgan,^[d] Sylvie Condon,^[d] Eric Léonel,^[d] Michel Evain,^[e] Jacques Lebreton,^[a] Denis Jacquemin,^[f] Muriel Pipelier,^[a] and Didier Dubreuil^{*[a]}

chem_201000859_sm_miscellaneous_information.pdf

Supporting Information:

Table of contents

Page S2	General Methods
Page S3	Theoretical studies
Page S4	X-Ray crystallographic studies
Page S5	Additional data on the electrochemical process
Page S6	NMR spectra of 11c , 17 , 13 , 14 , 2a , 2b , 2c , 1b and 1c

General Methods:

Chemicals: Solvents were purified and dried by standard methods prior to use.^[1] ZnCl₂ (0.7 molL⁻¹ in THF, *n*BuLi (2.5 molL⁻¹ in hexanes) were purchased from Acros company.

Electroreduction materials: Cyclic voltammetry experiments and preparative electrolysis were performed using a potentiostat-galvanostat EGG PARC Model 273 controlled by the Echem software. In cyclic voltammetry, a conventional three-electrode system was used with a glassy carbon working electrode, a saturated calomel reference electrode (SCE) and a platinum wire counter electrode. Preparative electrolysis were carried out under cathodic potential (E_w) in a concentric cylindrical cell with two compartments separated by a glass frit. A mercury pool electrode (diameter 4.7 cm) or a reticulated vitreous carbon (BAS-MF 2077) was used as cathode and a platinum plate as anode. A calomel saturated electrode in a Luggin-capillary (filed with the supporting electrolyte) was placed close to 5 mm to the working electrode and used as reference.

General analytical materials: All reactions were monitored by TLC on commercially available pre-coated plates (Kieselgel 60 F₂₅₄) and the products were visualized under UV light ($\lambda = 254$ nm for all compounds and 366 nm for *bis*-pyrrole derivatives **1a-c**) and with the Mohr test (FeSO₄ 10% in water). Kieselgel 60, 230-400 mesh (Merck), was used for column chromatography. Melting points were measured on a RCH microscope (C. Reichert), with a heating plate KOFLER. ¹H and ¹³C NMR spectra were recorded on a Bruker AC 300 at room temperature, using CDCl₃ or [D₆]DMSO as solvent, with the residual solvent signal as the internal reference ($\delta = 7.27$ and 77.0 ppm or $\delta = 2.50$ and 39.5 ppm respectively). The following abbreviations are used to describe peak patterns when appropriate: s (singlet), d (doublet), t (triplet), q (quadruplet), m (multiplet), and br (broad). The mass spectra were recorded on a DSQ Thermoelectron apparatus by electronic impact (70eV), either by direct introduction or by GC-MS coupling. High Resolution Mass Spectra (HRMS) were recorded by chemical ionisation on quadripolar spectrometers KRATOS MS 80RF or Micromasse Q T of 1. The electrospray was done by using Na⁺ or K⁺ ions. FTIR spectra were obtained in the 500-4000 cm⁻¹ range on a Bruker Vector 22 FT-IR spectrometer. Elemental analyses were performed at the "Service central d'analyse-CNRS" in Solaize (France).

UV/Vis and fluorescence instruments: Ground state absorption spectra were recorded at room temperature on a Perkin-Elmer Lambda 25 spectrophotometer. Fluorescence excitation and emission spectra were obtained using a Perkin-Elmer LS 55 spectrofluorimeter. All spectra were recorded in quartz cuvettes of 1 x 1 cm cross section at room temperature.

Evaluation of cytotoxicity: The cytotoxicity was studied on 6 distinct cell lines obtained from the european ECAC collection and on skin diploid fibroblasts which were provided by BIOPREDIC International Company. They included two human colon carcinoma cells Caco2 and HCT 116 representative of two distinct differentiated and highly colon tumorigenic tumors respectively, a differentiated highly growing HUH7 hepatocarcinoma cells, the MDA-MB231 breast, NCI lung and PC3 prostate tumor cells. They were grown according to the providers recommendations. The Cytotoxicity assay was based on an automated imaging analysis as followed: 4 x 10³ cells were seeded in 96 multiwell plates and led for 24h for attachment, spreading and growth. Then, they were exposed for 24 and 48h to increasing concentrations of the compounds, ranging from 0.1 to 25 μ M in a final volume of 80 μ l of culture medium. They were fixed with 4% paraformaldehyde solution and nuclei were stained with Hoechst 3342 and counted according to automated imaging quantification. 4 pictures per well were obtained with a high speed camera and statistical analyses were established using the Simple PCI software. In addition, imaging analysis allowed detection of possible cell morphology changes.

Theoretical studies:

All calculations have been performed with the Gaussian09 program^[2] using standard procedures, algorithms and default thresholds, except when noted. The selected computational procedure has been proven to be suitable for the simulation of the electronic transition energies of most organic compounds,^[3,4] and we only summarize the calculation process herein. In the first computational step we have optimized, with the PBE0/6-311G(d,p)^[5] method the ground-state geometry of all derivatives. These analytic force minimizations have been carried out until the *rms* force is smaller than 1×10^{-5} a.u. (so-called *tight* threshold). In a second stage, the vibrational modes have been computed at the same level of theory, so to ensure the presence of true minima. In the last step, the first ten or twenty low-lying excited-states have been determined within the vertical TD-DFT approximation using the diffuse-containing 6-311+G(2d,p) atomic basis set, that yields converged spectral values, at least for low-lying excited-states.^[4] The TD-DFT simulations have been performed with the CAM-B3LYP functional,^[6] as this range-separated hybrid provides a consistent description of excited-state energies.^[7,8] Test TD-PBE0 calculations have been performed as well for **2b** and yield the same qualitative conclusions, though, as could be expected,^[8] PBE0 (CAM-B3LYP) tends to slightly underestimate (overestimate) the transition energies. The SCF convergence criterion has been systematically tightened to, at least, 10^{-8} a.u. For the simulation of UV/Vis. spectra, the medium effects have been included at all three computational stages, by means of the Polarizable Continuum Model (PCM)^[9] in its non-equilibrium approximation for the TD-DFT step. The solvent selected is CH₂Cl₂, in order to match experimental conditions. For this aprotic medium, the PCM approximation is expected to restore the large majority of environmental effects. We have selected the UAKS (United Atom Kohn-Sham) radii to build the cavity lodging the molecule, as these radii are optimal for DFT calculations. The complexation energy of the water molecule inside **1b** has been estimated at the PBE0/6-311G(d,p) level using the well-known counterpoise correction of the total (internal) energy.

X-ray crystallographic studies:

Dipyrrole **1b** crystallizes from mixture *n*hexane/CHCl₃ in ratio of 4:1. Single-crystal X-ray data were collected at $T = 213$ K on a Rigaku MM07 rotating anode diffractometer using CuK α radiation. The structure was solved by direct methods with SHELXD and refined by full-matrix least-squares on F^2 using the SHELX-97 programs.^[10] Non-hydrogen atoms were refined anisotropically, and hydrogen atoms were placed in calculated position refined using idealized geometries (riding model) and assigned fixed isotropic displacement parameters.

Dipyrrole **1c** crystallizes from mixture *n*hexane/CHCl₃ in ratio of 4:1. A crystal of **1c** was mounted at the tip of Lindemann capillary by means of solvent free glue. Single-crystal X-ray data were collected at $T = 293$ K on a Bruker-Nonius Kappa CCD diffractometer, using graphite-monochromatized MoK-L_{2,3} radiation ($\lambda = 0.71073$ Å). Data were corrected for Lorentz-polarization effects and absorption corrections applied using a Gaussian integration. Friedel pairs have been merged. The structure was solved with the Sir2004 direct methods^[11] and subsequent calculations were carried out with the Jana2000 program package.^[12] All non-hydrogen atoms were refined anisotropically and hydrogen atoms were introduced with geometrical constraints and riding atomic displacement parameters.

Complex **1b-Cu^{II}** crystallizes from CHCl₃/MeOH. Single-crystal X-ray data were collected at $T = 213$ K on a Rigaku MM07 rotating anode diffractometer using CuK α radiation. The structure was solved by direct methods with SHELXD and refined by full-matrix least-squares on F^2 using the SHELX-97 programs.^[10] Non-hydrogen atoms were refined anisotropically, and hydrogen atoms were placed in calculated position refined using idealized geometries (riding model) and assigned fixed isotropic displacement parameters.

Crystal data for the three molecular compounds are shown in Table 1.

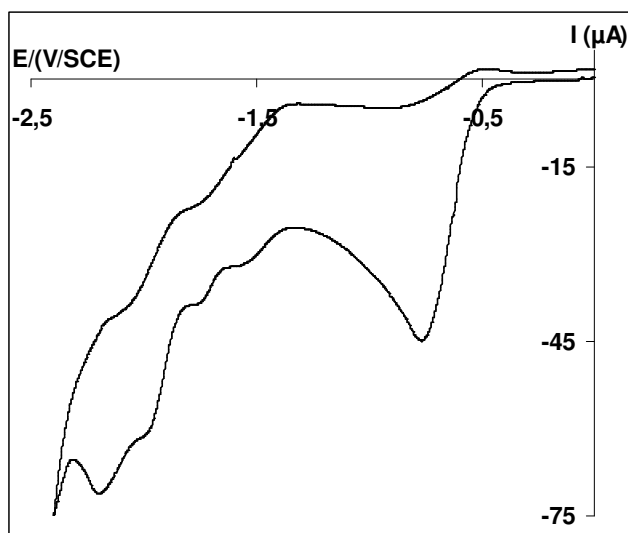
Table 1. Summary of crystal data of **1b**, **1c** and **1b-Cu^{II}**

	1b	1c	1b-Cu^{II}
Chemical formula	C ₂₅ H ₂₃ N ₅ O	C ₂₇ H ₂₇ N ₅ O	C ₂₈ H ₂₅ ClCu ₂ N ₅ O ₃
Formula weight	409.48	437.5	642.06
Temperature (K)	213(2)	293	213(2)
Wavelength (Å)	1.54178	0.71069	1.54178
Crystal system	Monoclinic	Monoclinic	Orthorhombic
Space group	C _{2/c}	C _{2/c}	Pm2(1)n
Unit cell dimensions (Å)	a = 23.478(1) b = 12.471(2) c = 7.200(2)	a = 25.2642(17) b = 12.6325(12) c = 7.2257(6)	a = 18.262(1) b = 19.025(2) c = 7.543(2)
Volume (Å ³)	2091.8	2305.8	2620.7
Z	4	4	4
Density (gcm ⁻³)	1.300	1.2607	1.627
Absorption coefficient (mm ⁻¹)	0.656	0.79	3.280
F(000)	864	928	1308
Crystal size (mm)	0.2 x 0.2 x 0.2	0.24 x 0.14 x 0.05	0.2 x 0.2 x 0.2
θ_{max} (°)	72.19	29.21	71.70
Observed reflections	3839	25391	15359
Unique reflections	1804	3074	5228
Refinement method	Full-matrix least-squares on F^2		Full-matrix least-squares on F^2
Goodness-of-fit on F^2	1.053	2.05	1.170
Final R indices	R1 = 0.0805, wR2 = 0.2327	R1 = 0.0903, wR2 = 0.1894	R1 = 0.1273, wR2 = 0.3558

CCDC-764884 (**1b**), -764885 (**1b-Cu^{II}**) and -770696 (**1c**) contains the supplementary crystallographic data for this paper. These data can be obtained free of charge from The Cambridge Crystallographic Data Centre via www.ccdc.cam.ac.uk/data_request/cif.

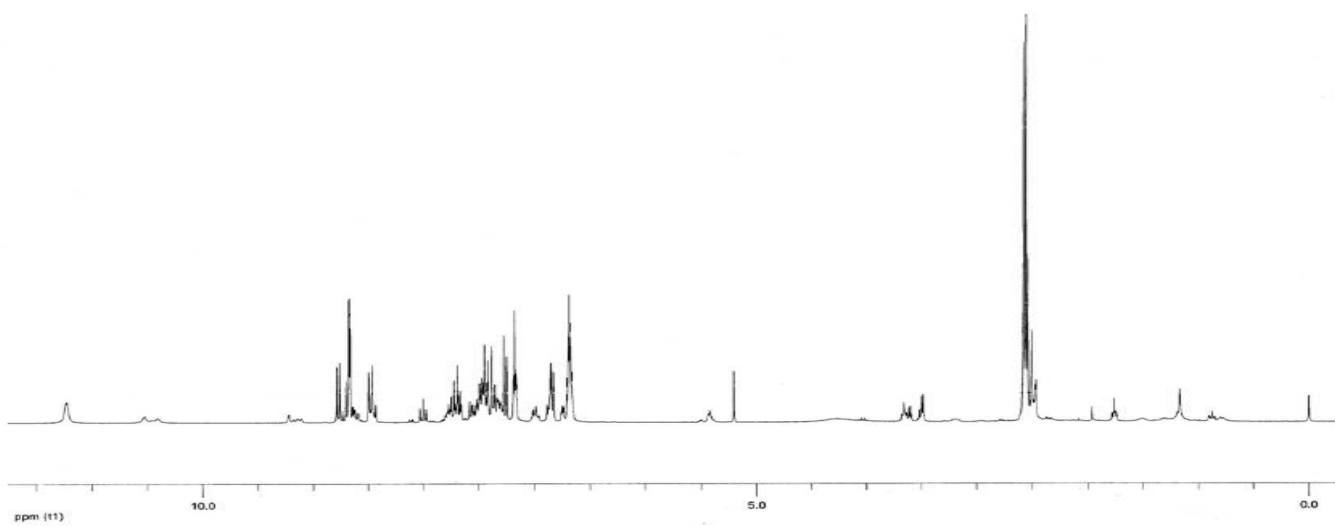
Additional data on the electrochemical process: Electrochemical ring contractions and pyridyl-pyrrole strands synthesis

Cyclic voltammogram of 2b ($C = 4 \times 10^{-3} \text{ molL}^{-1}$) in a DMF, at a glassy carbon electrode ($v = 0.1 \text{ Vs}^{-1}$), in presence of a support electrolyte ($n\text{Bu}_4\text{NBr } 0.10 \text{ molL}^{-1}$) and a source of protons (H_2SO_4 16.0 equiv).



^1H NMR spectrum of the crude mixture obtained when the electroreduction of **2b** was run at the potential of the first reduction peak after consumption of 4 Fmol^{-1} . Similar spectrum was obtained when the experiment is achieved at the second reduction peak limiting the electron source to 4 Fmol^{-1} .

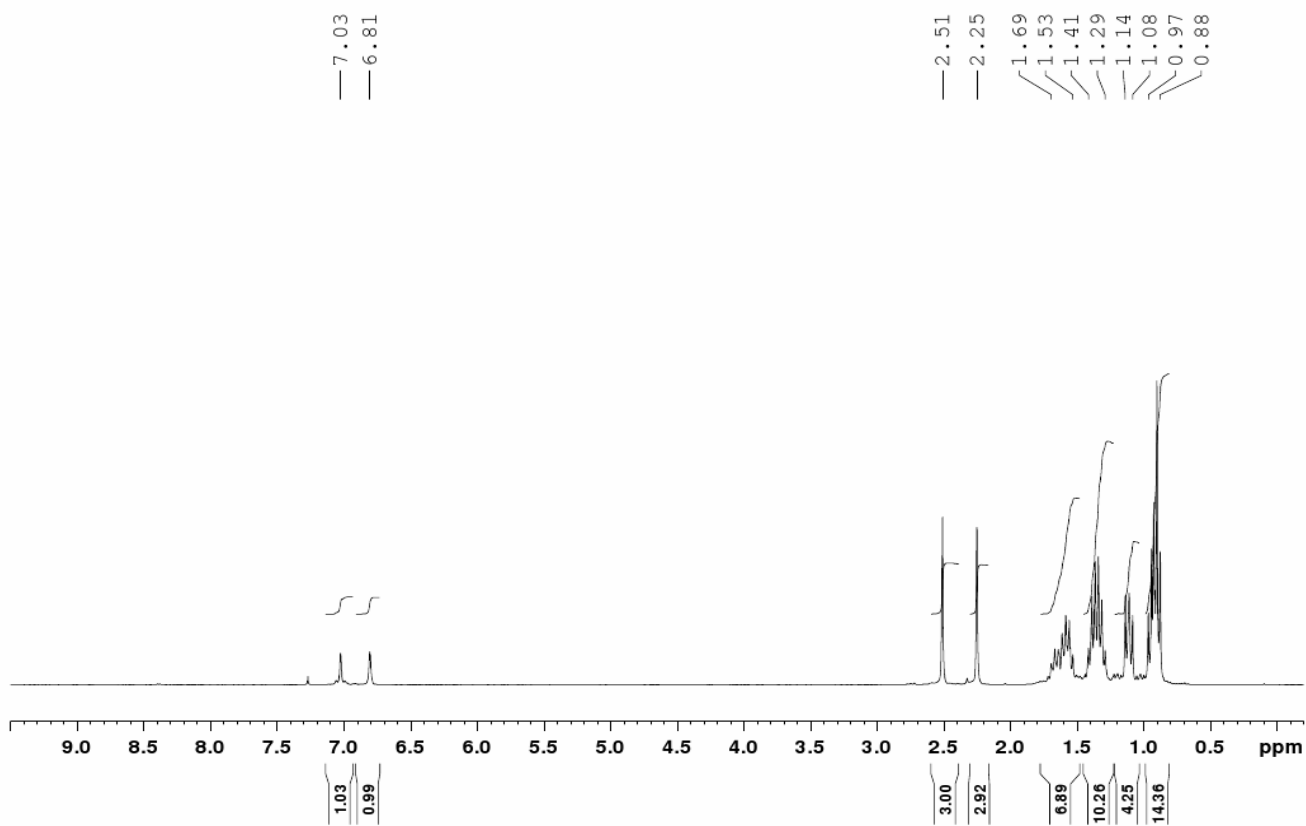
^1H NMR (CDCl_3):



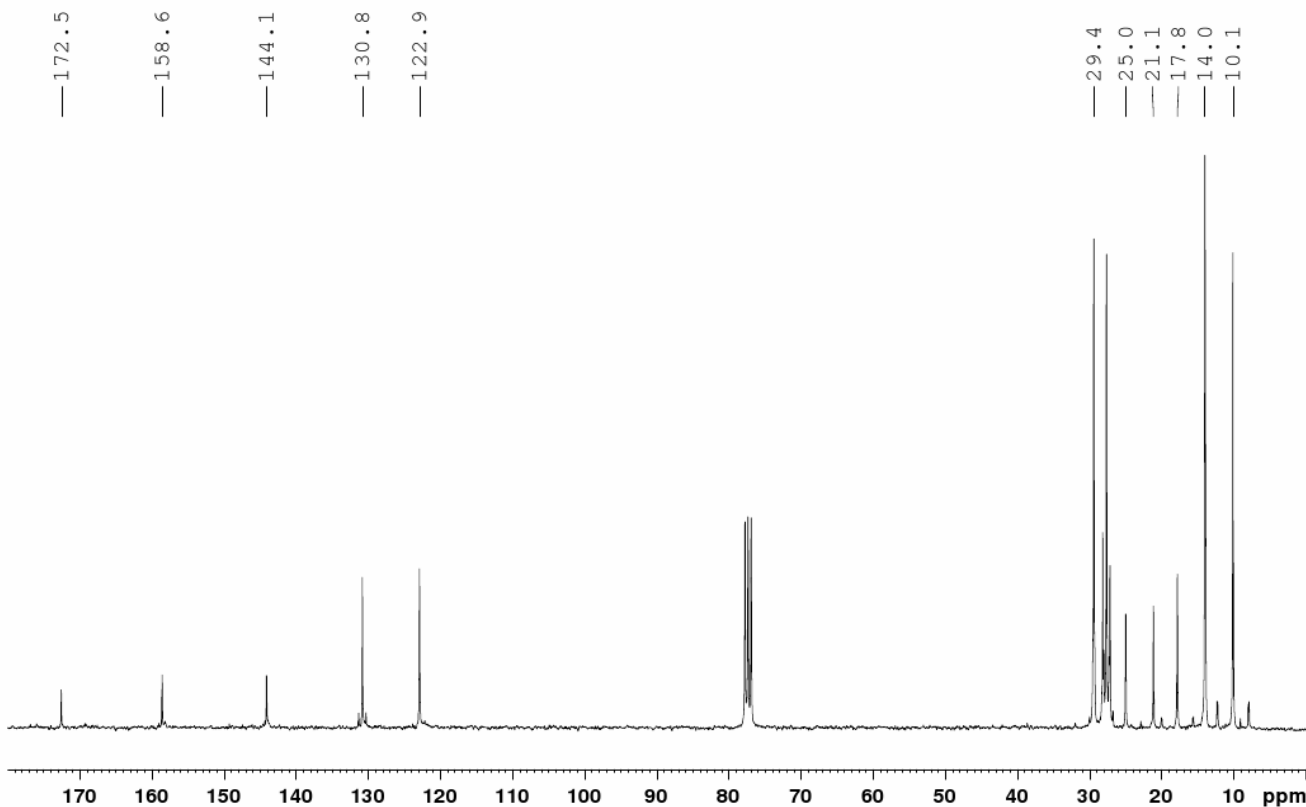
^1H and ^{13}C NMR spectra of all synthetic compounds:

2,4-dimethyl-6-(tributylstannyl)pyridine (11c):

^1H NMR (CDCl_3):

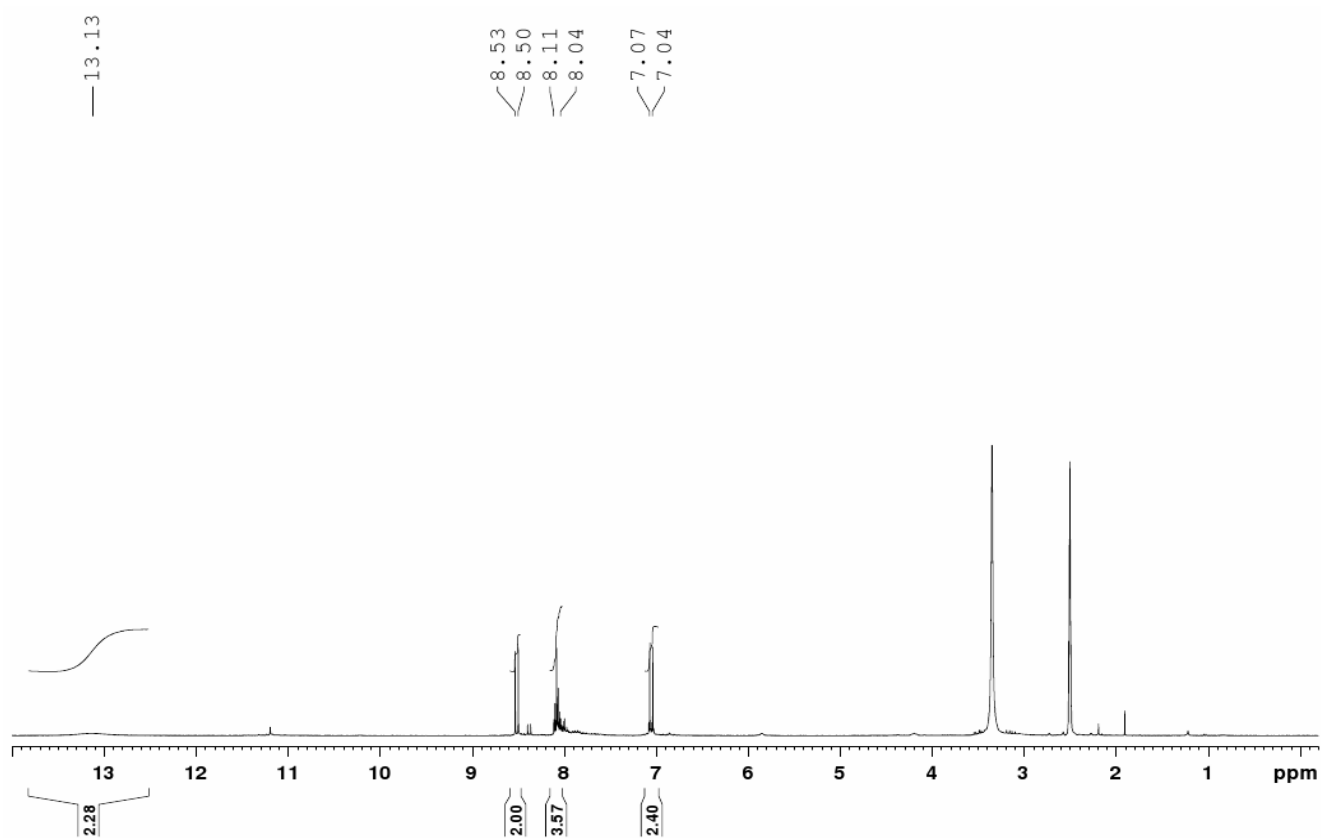


^{13}C NMR (CDCl_3):

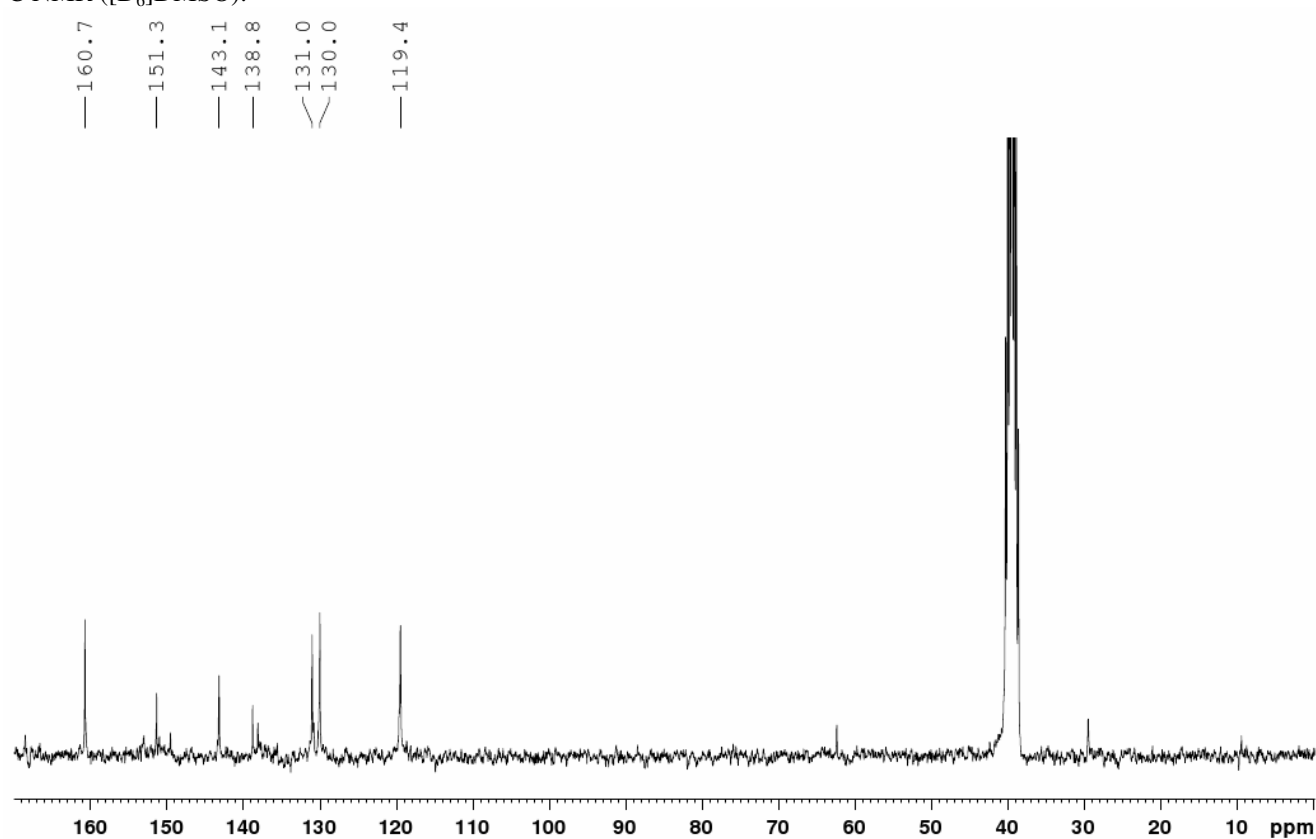


6,6'-(pyridine-2,6-diyl)dipyridazin-3(2H)-one (17):

^1H NMR ($[\text{D}_6]\text{DMSO}$):

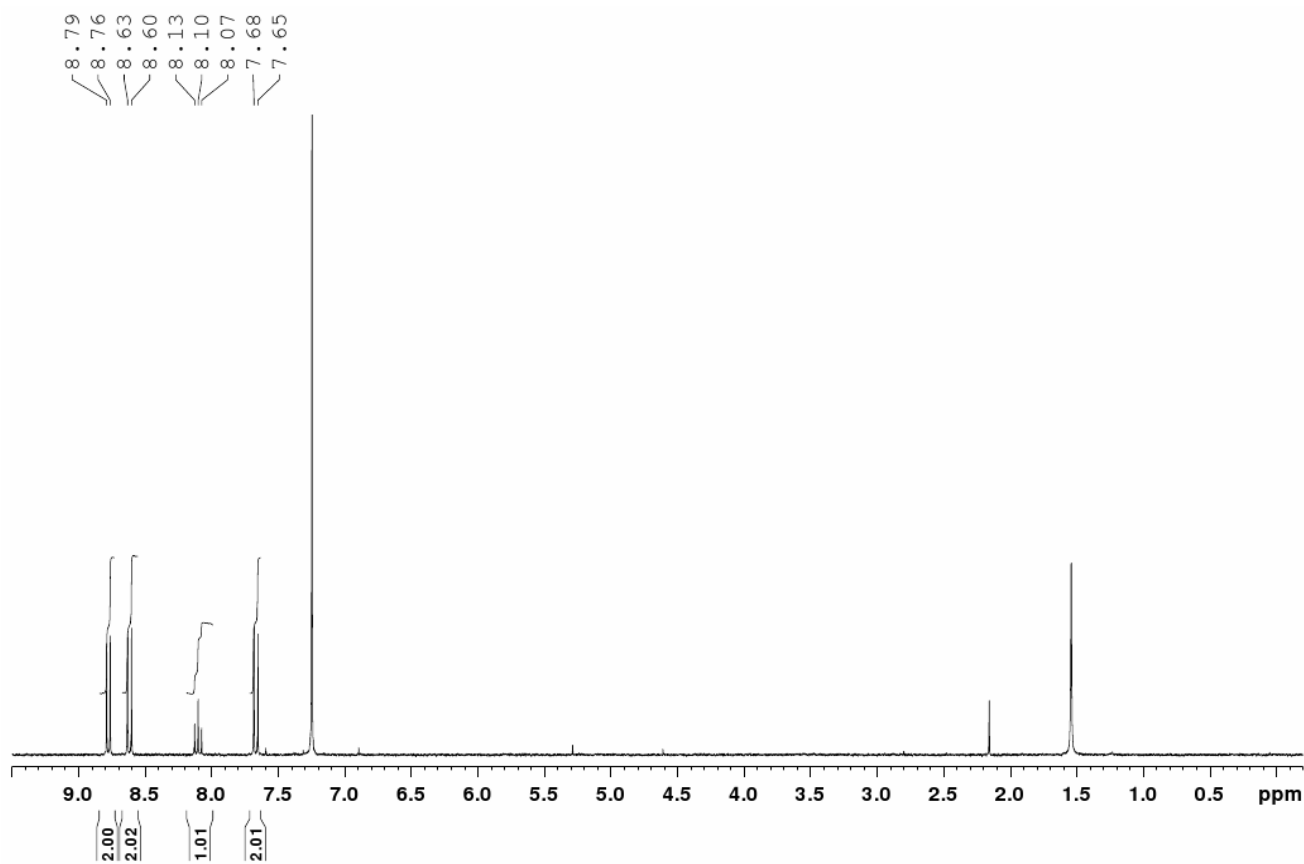


^{13}C NMR ($[\text{D}_6]\text{DMSO}$):

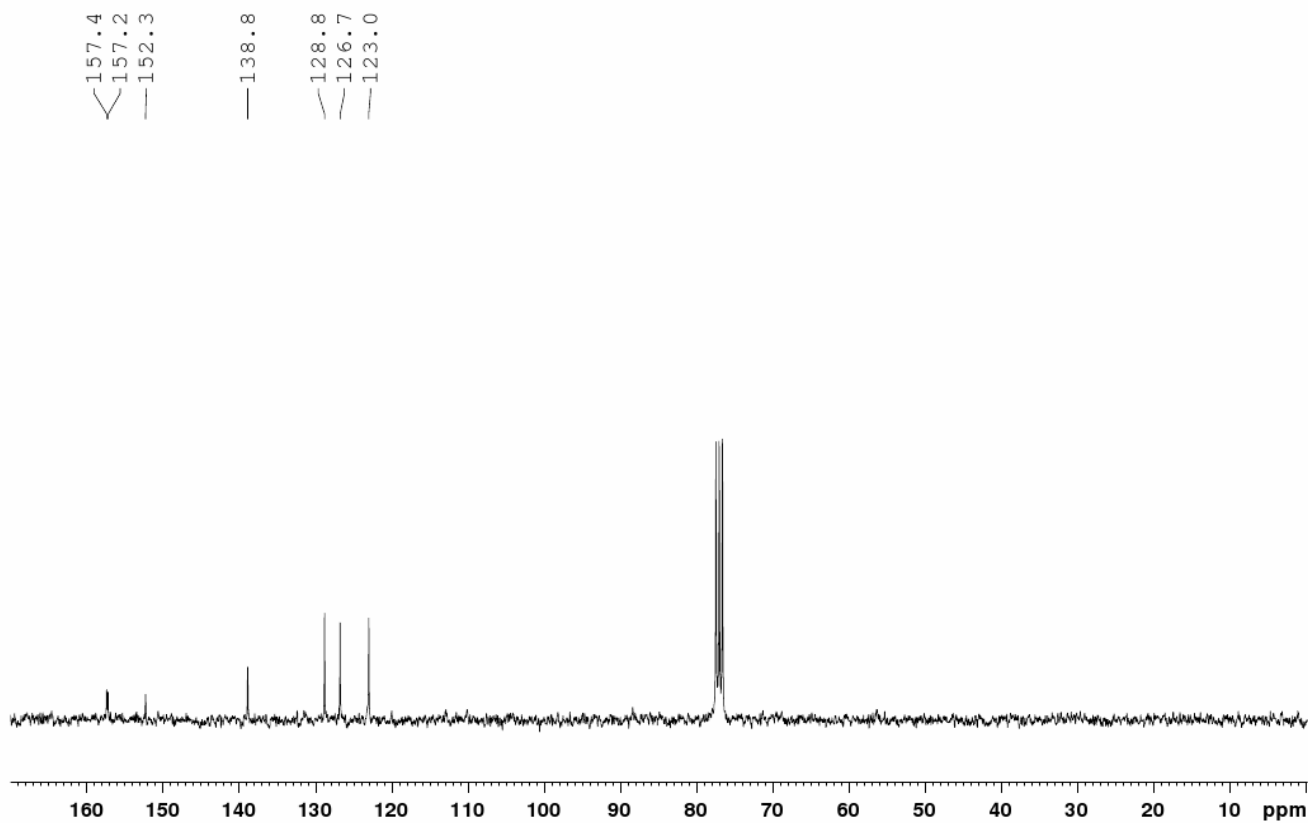


2,6-bis(6-chloropyridazin-3-yl)pyridine (13):

¹H NMR (CDCl₃):



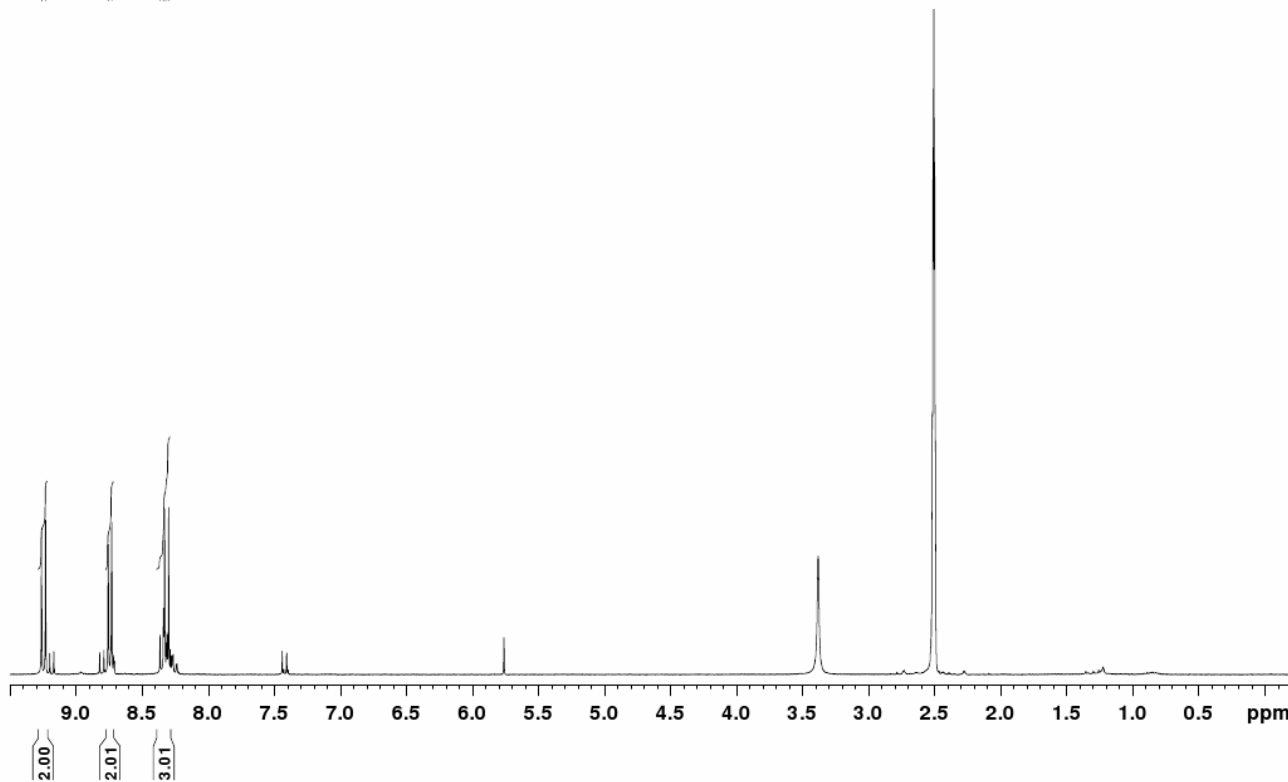
¹³C NMR (CDCl₃):



2,6-bis(6-trifluoromethanesulfonylpyridazin-3-yl)pyridine (14):

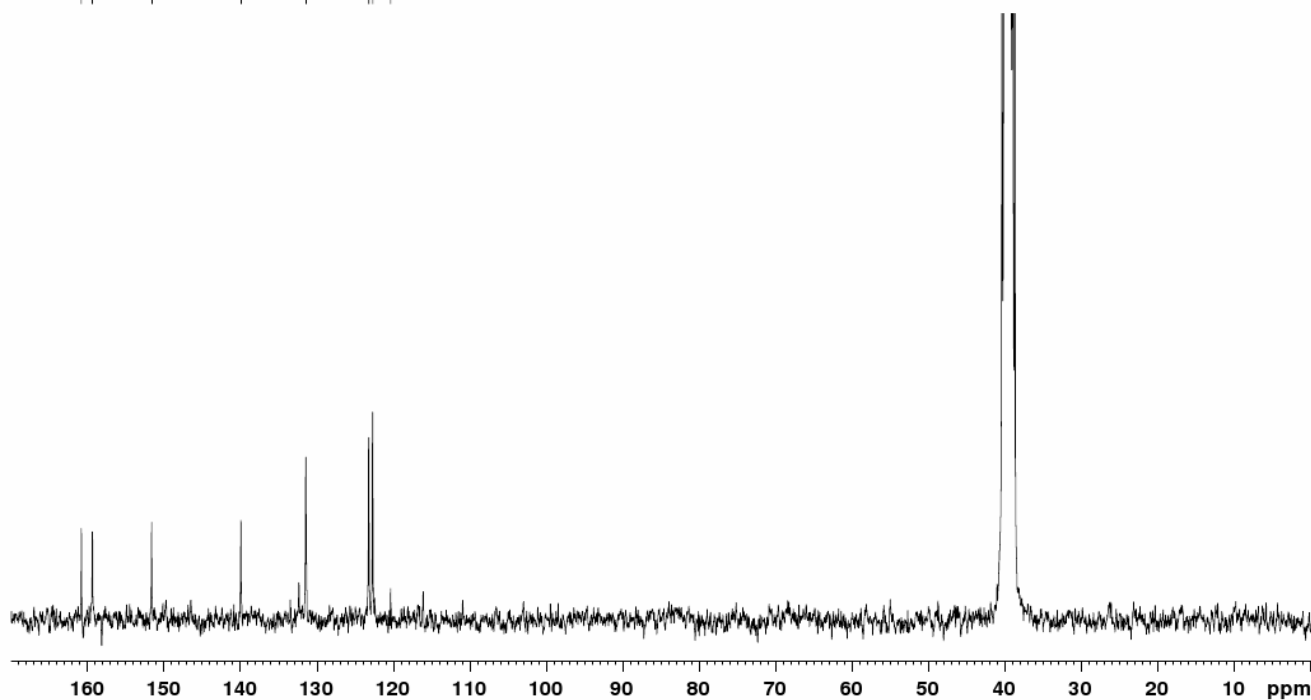
$^1\text{H NMR}$ ($[\text{D}_6]\text{DMSO}$):

9.258
9.228
8.756
8.729
8.364
8.338
8.329
8.311
8.299



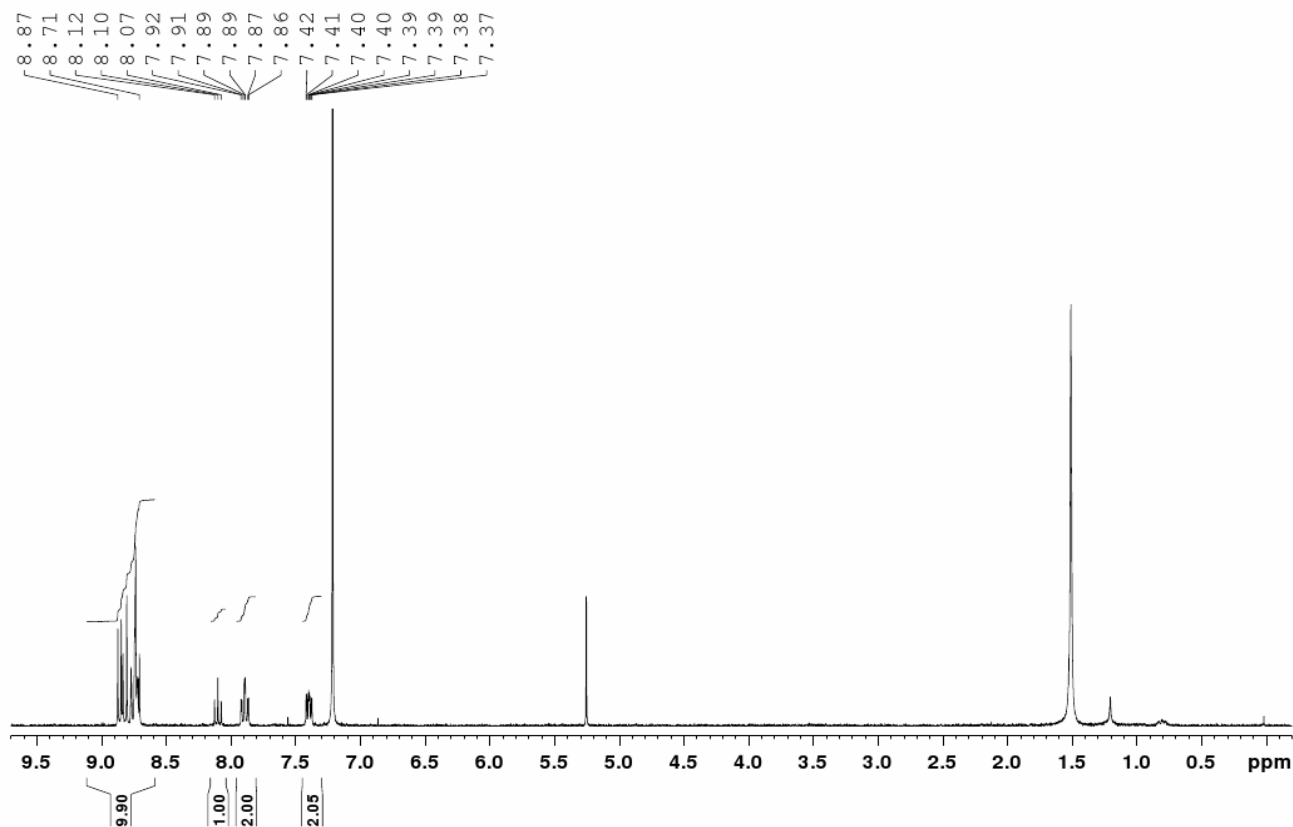
$^{13}\text{C NMR}$ ($[\text{D}_6]\text{DMSO}$):

160.8
159.3
151.6
139.9
131.4
123.2
122.7
120.3

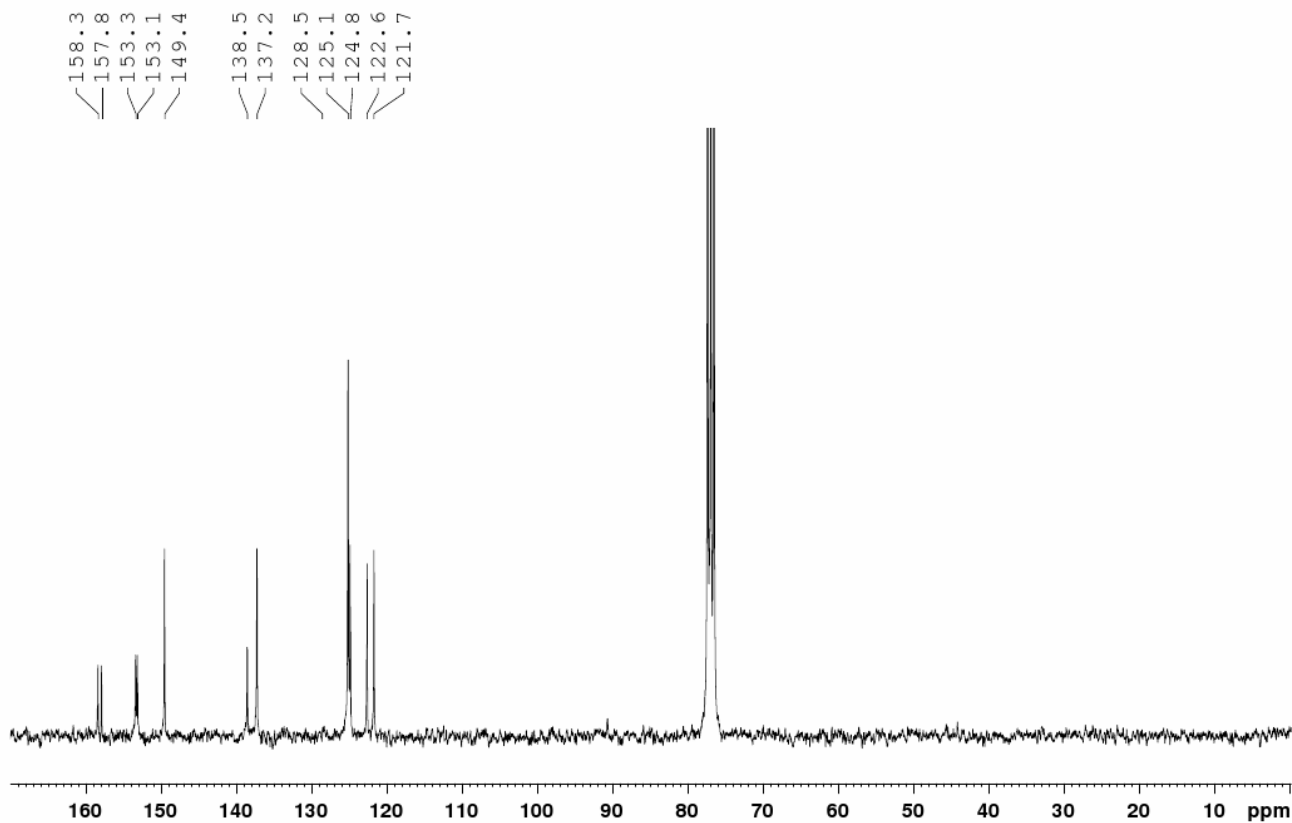


2,6-bis[6-(pyridin-2-yl)pyridazin-3-yl]pyridine (2a):

¹H NMR (CDCl₃):

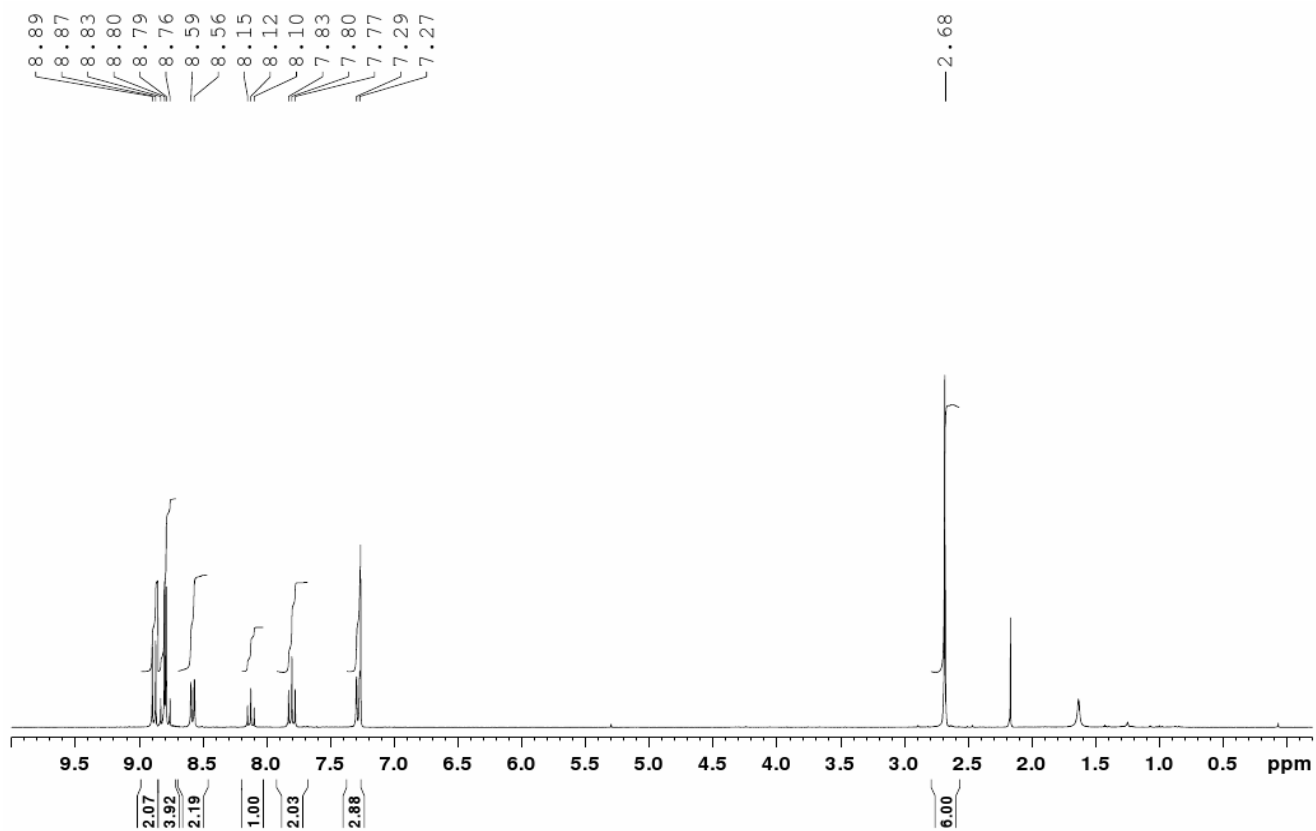


¹³C NMR (CDCl₃):

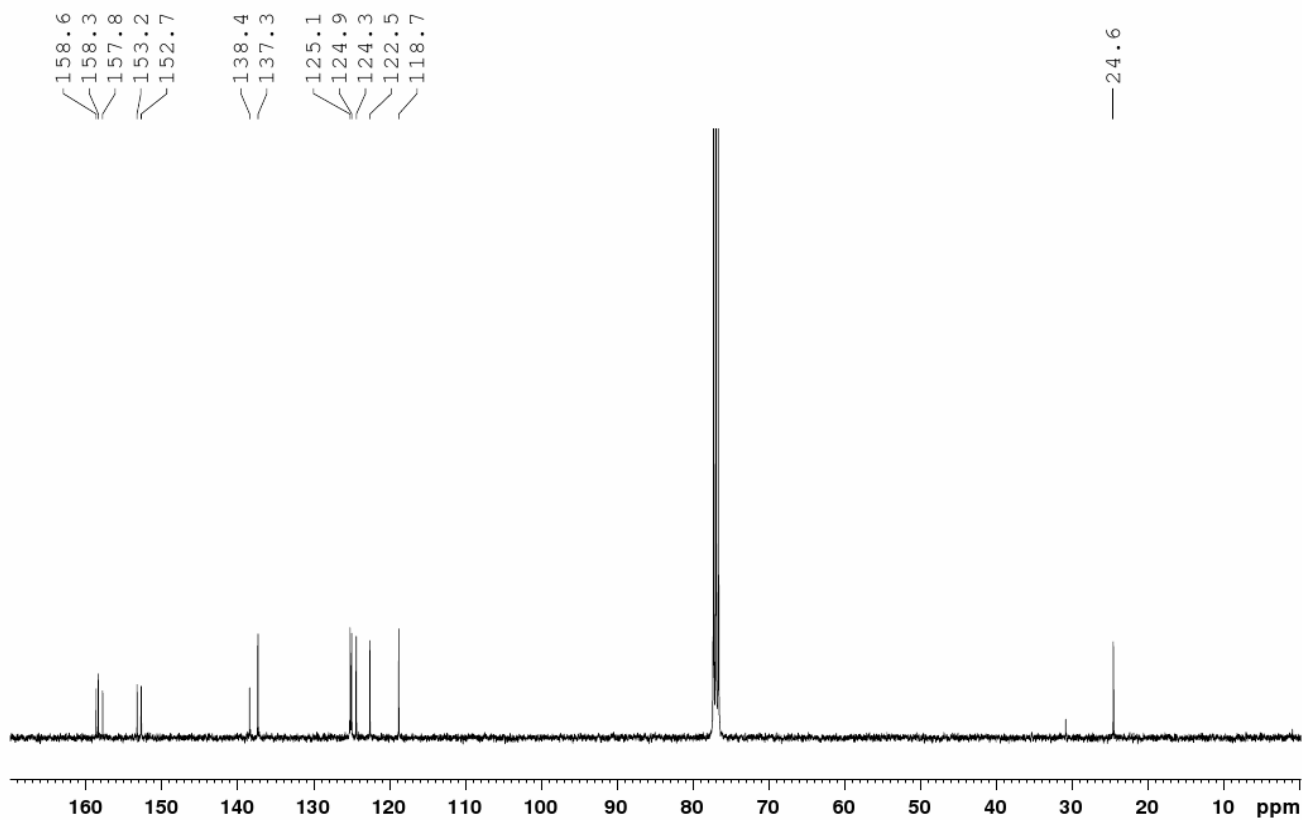


2,6-bis(6-(6-methylpyridin-2-yl)pyridazin-3-yl)pyridine (2b)

$^1\text{H NMR}$ (CDCl_3):

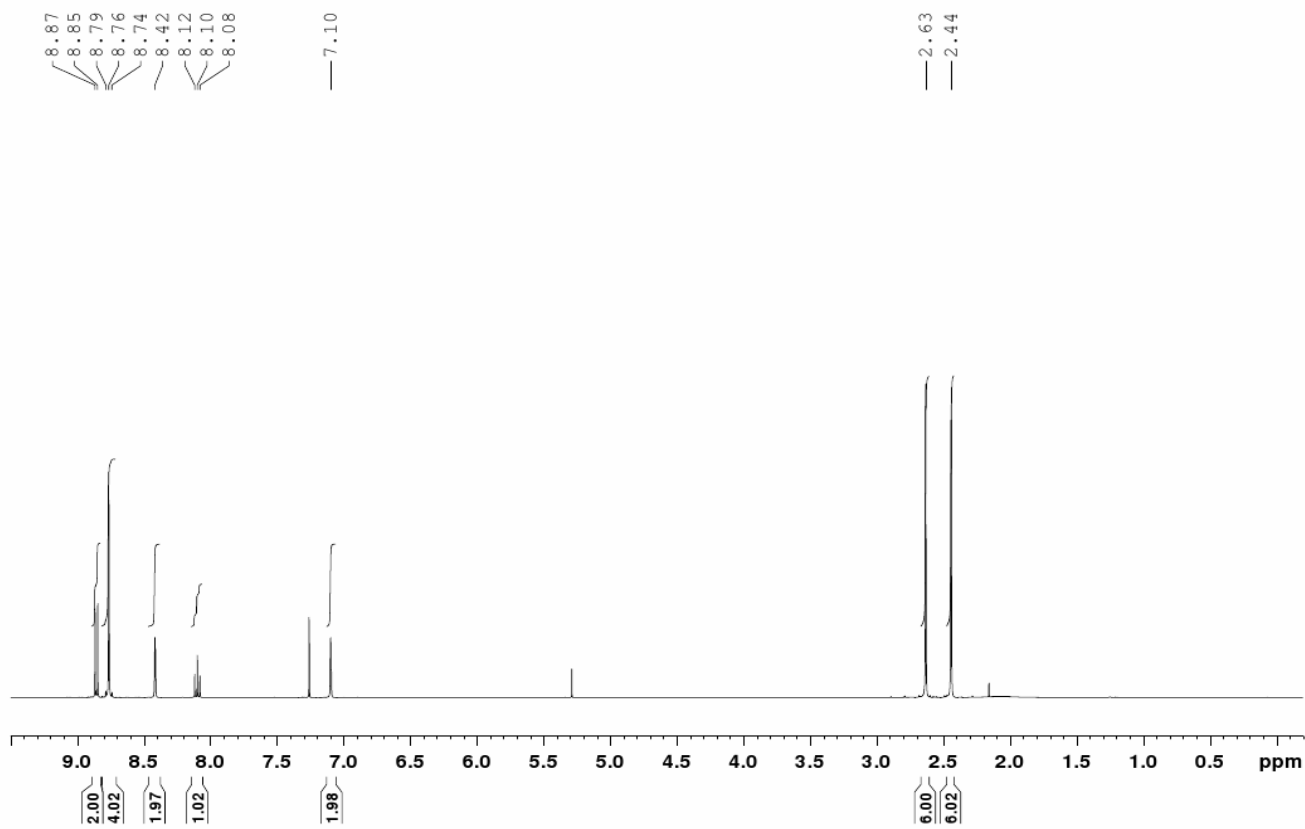


$^{13}\text{C NMR}$ (CDCl_3):

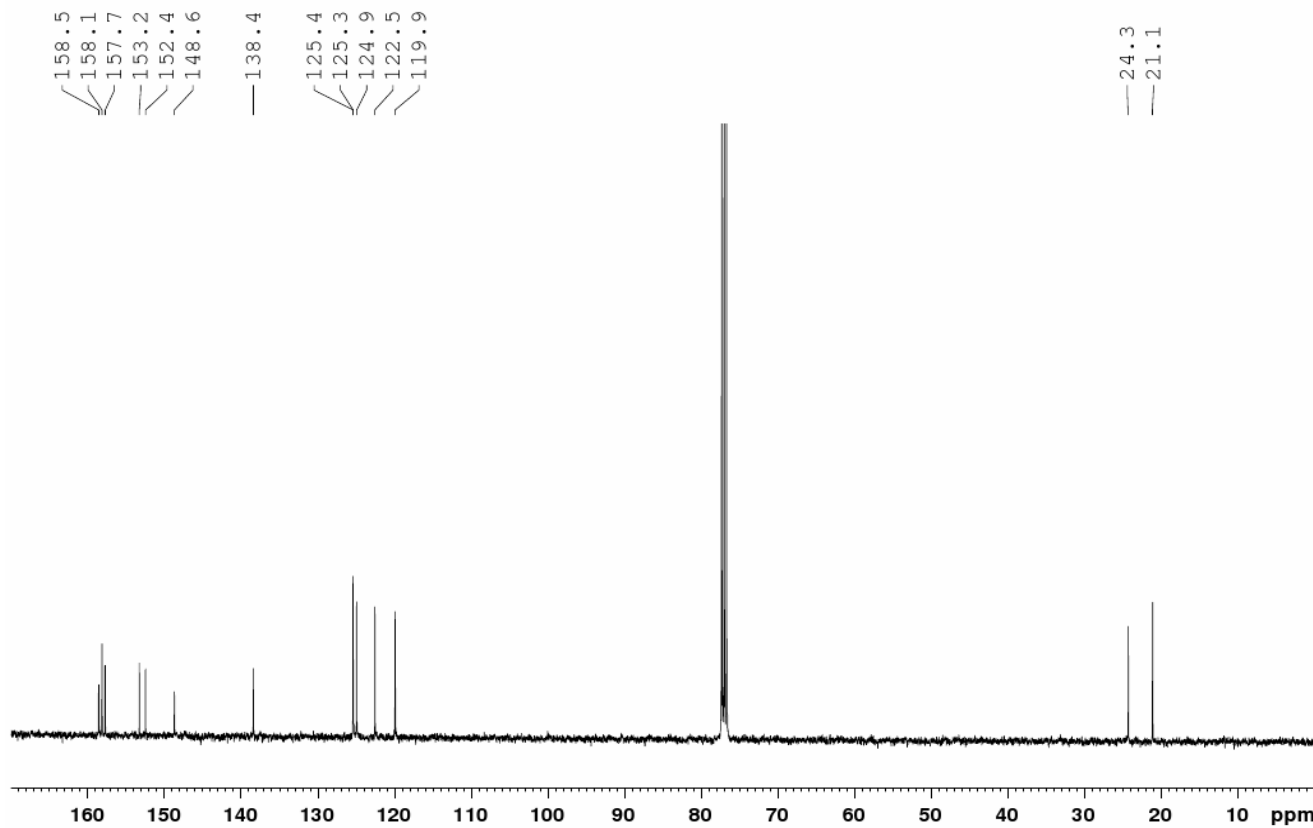


2,6-bis[6-(4,6-dimethylpyridin-2-yl)pyridazin-3-yl]pyridine (2c):

^1H NMR (CDCl_3):

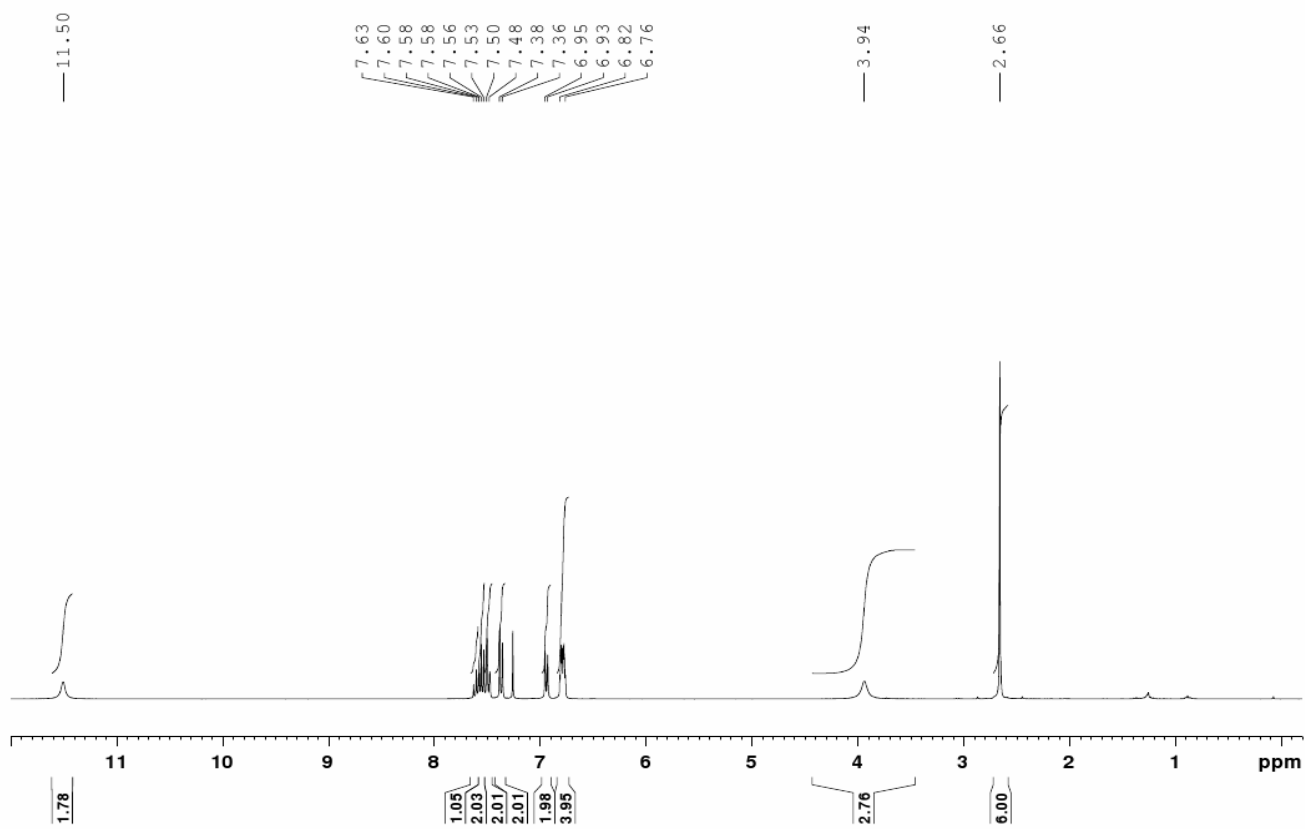


^{13}C NMR (CDCl_3):

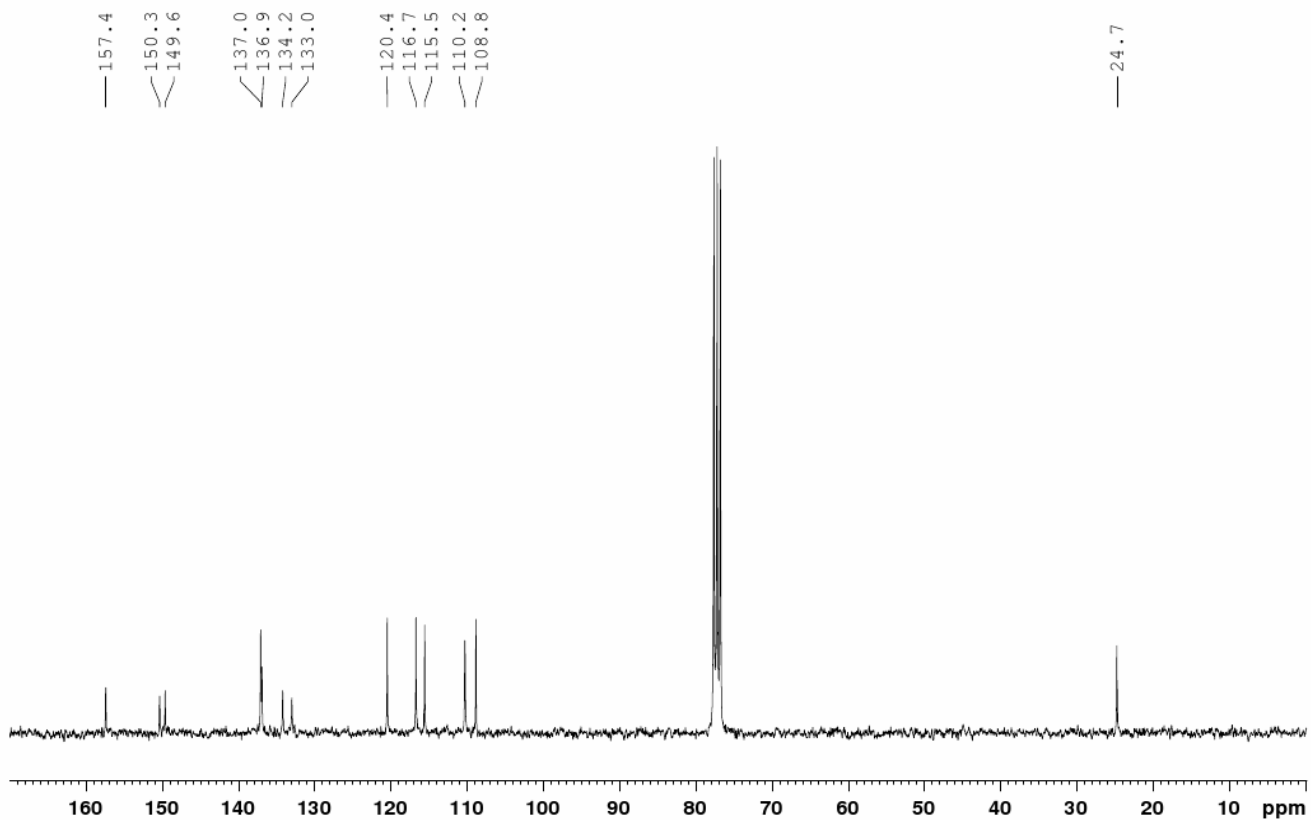


2,6-bis[5-(6-methylpyridin-2-yl)pyrrol-2(1H)-yl]pyridine (1b):

^1H NMR (CDCl_3):

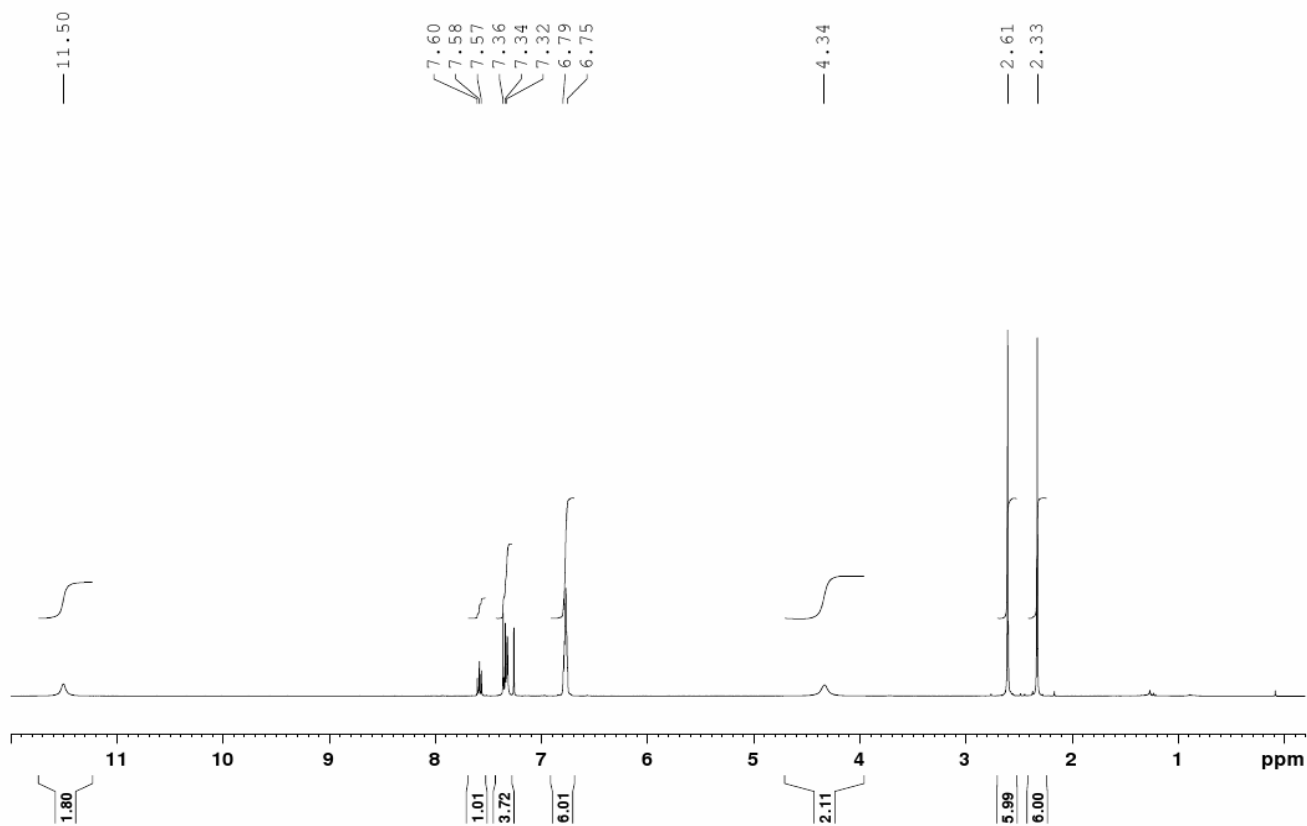


^{13}C NMR (CDCl_3):

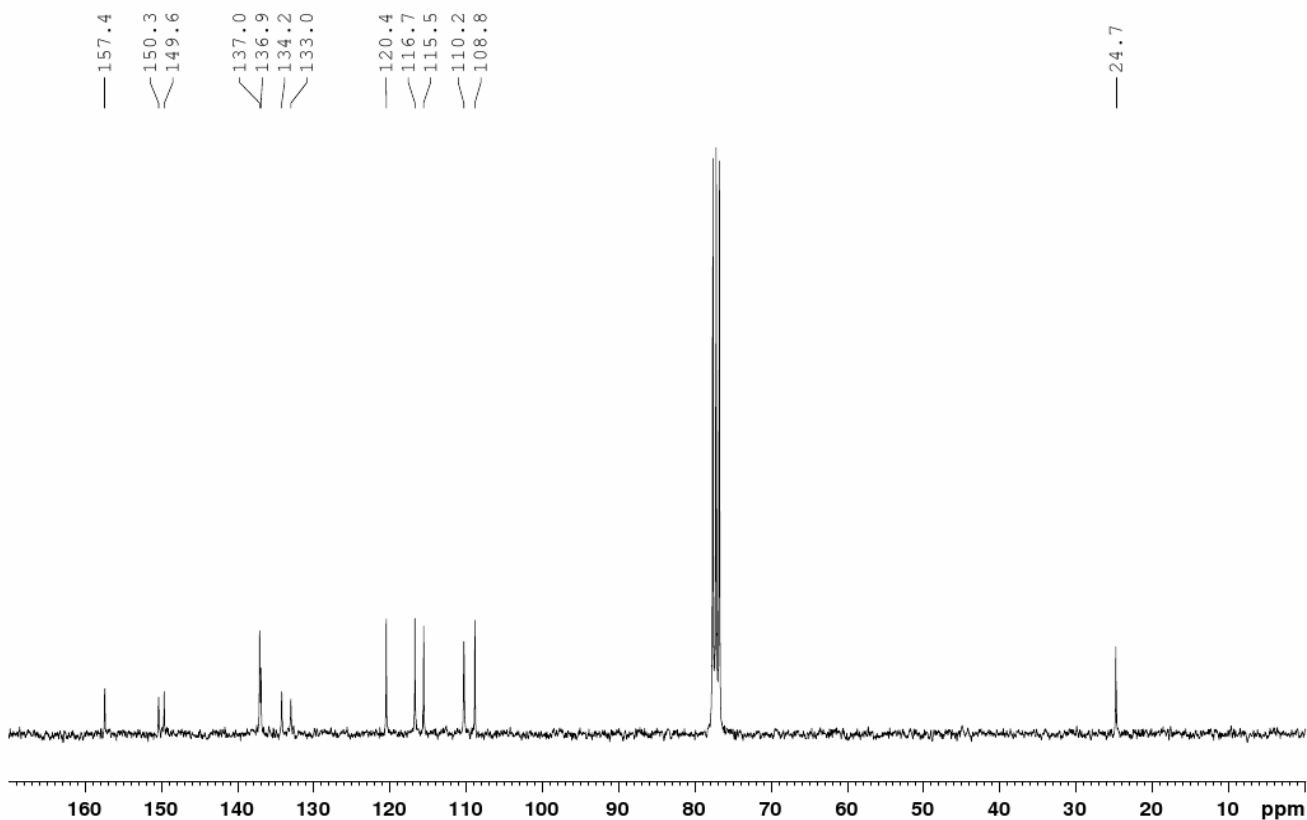


2,6-bis[5-(4,6-dimethylpyridin-2-yl)pyrrol-2(1H)-yl]pyridine (1c):

^1H NMR (CDCl_3):



^{13}C NMR (CDCl_3):



-
- [1] D. D. Perrin, W. L. F. Amarego, *Purification of Laboratory Chemicals*, Pergamon, Oxford, **1988**.
- [2] M. J. Frisch, G. W. Trucks, H. B. Schlegel, G. E. Scuseria, M. A. Robb, J. R. Cheeseman, J. A. Montgomery, J. T. Vreven, K. N. Kudin, J. C. Burant, J. M. Millam, S. S. Iyengar, J. Tomasi, V. Barone, B. Mennucci, M. Cossi, G. Scalmani, N. Rega, G. A. Petersson, H. Nakatsuji, M. Hada, M. Ehara, K. Toyota, R. Fukuda, J. Hasegawa, M. Ishida, T. Nakajima, Y. Honda, O. Kitao, H. Nakai, M. Klene, X. Li, J. E. Knox, H. P. Hratchian, J. B. Cross, C. Adamo, J. Jaramillo, R. Gomperts, R. E. Stratmann, O. Yazyev, A. J. Austin, R. Cammi, C. Pomelli, J. W. Ochterski, P. Y. Ayala, K. Morokuma, G. A. Voth, P. Salvador, J. J. Dannenberg, V. G. Zakrzewski, S. Dapprich, A. D. Daniels, M. C. Strain, O. Farkas, D. K. Malick, A. D. Rabuck, K. Raghavachari, J. B. Foresman, J. V. Ortiz, Q. Cui, A. G. Baboul, S. Clifford, J. Cioslowski, B. B. Stefanov, G. Liu, A. Liashenko, P. Piskorz, I. Komaromi, R. L. Martin, D. J. Fox, T. Keith, M. A. Al-Laham, C. Y. Peng, A. Nanayakkara, M. Challacombe, P. M. W. Gill, B. Johnson, W. Chen, M. W. Wong, C. Gonzalez, J. A. Pople, RevD.02 ed., Gaussian, Inc., Wallingford CT, **2004**.
- [3] V. Barone, A. Polimeno, *Chem. Soc. Rev.* **2007**, *36*, 1724-1731.
- [4] D. Jacquemin, E. A. Perpète, I. Ciofini, C. Adamo, *Acc. Chem. Res.* **2009**, *42*, 326-334.
- [5] C. Adamo, V. Barone, *J. Chem. Phys.* **1999**, *110*, 6158-6170.
- [6] T. Yanai, D. P. Tew, N. C. Handy, *Chem. Phys. Lett.* **2004**, *393*, 51-57.
- [7] M. J. G. Peach, C. R. Le Sueur, K. Ruud, M. Guillaume, D. J. Tozer, *Phys. Chem. Chem. Phys.* **2009**, *11*, 4465-4470.
- [8] D. Jacquemin, V. Wathélet, E. A. Perpète, C. Adamo, *J. Chem. Theory Comput.* **2009**, *5*, 2420-2435.
- [9] J. Tomasi, B. Mennucci, R. Cammi, *Chem. Rev.* **2005**, *105*, 2999-3093.
- [10] G. M. Sheldrick, *Acta Cryst.* **2008**, *A64*, 112-22.
- [11] M. C. Burla, R. Caliandro, M. Camalli, B. Carrozzini, G. L. Casciarano, L. De Caro, C. Giacovazzo, G. Polidori, R. Spagna, *J. Appl. Cryst.* **2005**, *38*, 381-388.
- [12] V. Petricek, M. Dusek, *JANA2000, a crystallographic computing system 2000*, Institute of Physics, Academy of Sciences of the Czech Republic, Prague, Czech Republic.